

Vacuum Friction in Rotating Particles

A. Manjavacas and F. J. García de Abajo*

Instituto de Óptica—CSIC, Serrano 121, 28006 Madrid, Spain
(Received 8 March 2010; published 8 September 2010)

We study the frictional torque acting on particles rotating in empty space. At zero temperature, vacuum friction transforms mechanical energy into light emission and produces particle heating. However, particle cooling relative to the environment occurs at finite temperatures and low rotation velocities. Radiation emission is boosted and its spectrum significantly departed from a hot-body emission profile as the velocity increases. Stopping times ranging from hours to billions of years are predicted for materials, particle sizes, and temperatures accessible to experiment. Implications for the behavior of cosmic dust are discussed.

DOI: 10.1103/PhysRevLett.105.113601

PACS numbers: 42.50.Wk, 41.60.-m, 45.20.dc, 78.70.-g

The radiation emitted by accelerated charges produces reaction forces acting back on them. For rotating charged particles (e.g., electric [1] and magnetic [2] dipoles), this gives rise to reaction torques [3]. Likewise, accelerated neutral bodies are known to experience friction because they emit light due to the absolute change in the boundary conditions of the electromagnetic field. This is the so-called Casimir radiation [4,5].

A spinning sphere presents a more challenging situation: its surface appears to be unchanged, although it experiences a centripetal acceleration. So, the question arises, does a homogeneous, neutral sphere emit light simply by rotating? Is such a particle slowing down when spinning in vacuum? We know the inverse process to be true: the angular momentum carried by light can be transformed into mechanical rotation of neutral particles [6]. However, this type of problem requires a delicate analysis, somehow related to the noncontact friction predicted to occur between planar homogeneous surfaces set in relative uniform motion [7], which is currently generating a heated debate [8].

In this Letter, we investigate the friction produced on rotating neutral particles by interaction with the vacuum electromagnetic fields. Friction is negligible in dielectric particles possessing large optical gap compared to the rotation and thermal-radiation frequencies. For other materials (e.g., metals), in contrast to previous predictions [9], we find nonzero stopping even at zero temperature. The dissipated energy is transformed into radiation emission and thermal heating of the particle, although cooling relative to the surrounding vacuum is shown to take place under very common conditions. We formulate a theory that describes these phenomena and allows us to predict experimentally measurable effects.

Theoretical description.—We consider an isotropic particle at temperature T_1 spinning with frequency Ω and sitting in a vacuum at temperature T_0 (see Fig. 1). The particle experiences a torque M by interaction with the surrounding radiation field and it is also capable of

exchanging photons, with net emission power P^{rad} . For simplicity, we assume the particle radius a to be small compared to the wavelength of the involved photons, so that we can describe it through its frequency-dependent polarizability $\alpha(\omega)$. Since the maximum frequency of exchanged photons is controlled by the rotation frequency and the thermal baths at temperatures T_0 and T_1 , this approximation implies that both $\Omega a/c$ and $k_B T_j a/c\hbar$ are taken to be small compared to unity. These conditions are fulfilled in very common situations (for instance, for $a = 50$ nm, one has $\Omega \ll 6 \times 10^3$ THz and $T_j \ll 4.6 \times 10^4$ K).

Friction originates in fluctuations of both (i) the vacuum electromagnetic field \mathbf{E}^{fl} and (ii) the particle polarization \mathbf{p}^{fl} . We calculate the emitted power from the work exerted by the particle dipole,

$$P^{\text{rad}} = -\langle \mathbf{E}^{\text{ind}} \cdot \partial \mathbf{p}^{\text{fl}} / \partial t + \mathbf{E}^{\text{fl}} \cdot \partial \mathbf{p}^{\text{ind}} / \partial t \rangle, \quad (1)$$

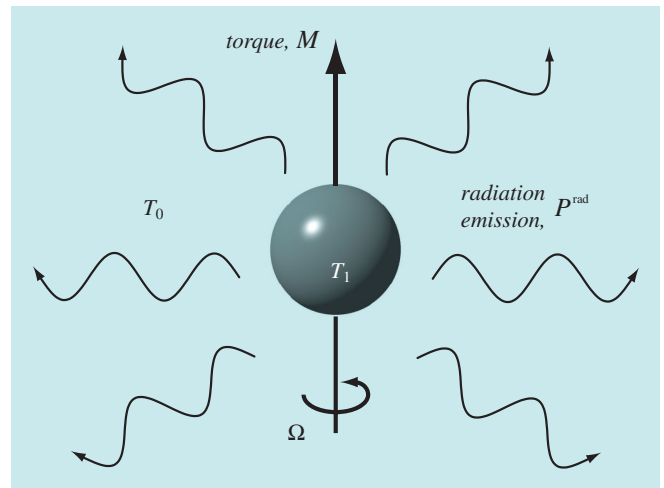


FIG. 1 (color online). Sketch of a spherical rotating particle and parameters considered in this work. The particle is at temperature T_1 and rotates with frequency Ω . The interaction with vacuum at temperature T_0 produces a frictional torque M and a radiated power P^{rad} .

where \mathbf{E}^{ind} is the field induced by \mathbf{p}^{fl} , and \mathbf{p}^{ind} is the dipole induced by \mathbf{E}^{fl} . Likewise, the torque is obtained from the action of the field on the dipole,

$$\mathbf{M} = \langle \mathbf{p}^{\text{fl}} \times \mathbf{E}^{\text{ind}} + \mathbf{p}^{\text{ind}} \times \mathbf{E}^{\text{fl}} \rangle. \quad (2)$$

The result is quadratic in \mathbf{E}^{fl} for contribution (i) and in \mathbf{p}^{fl} for contribution (ii). The brackets $\langle \rangle$ represent the average over these quadratic fluctuation terms, which we perform using the fluctuation-dissipation theorem (FDT) [10].

Rotational motion enters here through the transformation of the field and the polarization back and forth between rotating and lab frames. This is needed because the particle polarizability can only be applied in the rotating frame, in which the electronic and vibrational excitations participating in α are well defined and Ω independent. In contrast, the effective polarizability in the lab frame has a dependence on Ω . Further details of this formalism are given in [10]. The resulting radiated power reads (see [10] for a detailed derivation)

$$P^{\text{rad}} = \int_{-\infty}^{\infty} \hbar \omega d\omega \Gamma(\omega), \quad (3)$$

where

$$\Gamma(\omega) = (2\pi\omega\rho^0/3)\{2g_{\perp}(\omega - \Omega)[n_1(\omega - \Omega) - n_0(\omega)] + g_{\parallel}(\omega)[n_1(\omega) - n_0(\omega)]\} \quad (4)$$

is the spectral distribution of the rate of emission (when $\omega\Gamma > 0$) or absorption ($\omega\Gamma < 0$), $n_j(\omega) = [\exp(\hbar\omega/k_B T_j) - 1]^{-1}$ is the Bose-Einstein distribution function at temperature T_j ,

$$g_l(\omega) = \text{Im}\{\alpha_l(\omega)\} - \frac{2\omega^3}{3c^3} |\alpha_l(\omega)|^2$$

are odd functions of ω describing particle absorption for polarization either parallel ($l = \parallel$) or perpendicular ($l = \perp$) with respect to the rotation axis, and $\rho^0 = \omega^2/\pi^2 c^3$ is the free-space local density of photonic states. These results apply to particles with orthogonal principal axes of polarization, rotating around one of them, and with α_{\perp} given by the average of the polarizability over the remaining two orthogonal axes. The torque M takes a similar form,

$$M = - \int_{-\infty}^{\infty} d\omega \hbar \Gamma(\omega). \quad (5)$$

Incidentally, the g_{\parallel} term of Eq. (4) vanishes under the integral of Eq. (5), and furthermore, $M = 0$ for $\Omega = 0$. In the $T_0 = T_1 = 0$ limit, one has $n_j(\omega) = -\theta(\omega)$, from which we find the integrals to be restricted to the $(0, \Omega)$ range: only photons of frequency below Ω can be generated.

Unfortunately, Eqs. (1) and (2) do not account for radiative corrections coming from the elaborate motion of induced charges in the rotating particle. Although such corrections are insignificant for small particles, we incorporate them here for spheres in a phenomenological way

through the term proportional to $|\alpha|^2$ in Eq. (4), preceded by a coefficient chosen to yield $g_l = 0$ (and consequently, $M = 0$) in nonabsorbing particles [11]: internal excitations (i.e., absorption) are necessary to mediate the coupling between the rotational state and radiation [12]. Furthermore, we neglect magnetic polarization, which can be important for large, highly conductive particles [13].

Metallic particles.—This case is representative for absorbing particles. At low photon frequencies ω below the interband transitions region, metals can be well described by the Drude model, characterized by a dc electric conductivity σ_0 and a dielectric function $\epsilon = 1 + i4\pi\sigma_0/\omega$ [14]. For a spherical particle of radius a , we have $\alpha \approx a^3(\epsilon - 1)/(\epsilon + 2)$, and consequently

$$\text{Im}\{\alpha(\omega)\} \approx 3\omega a^3/4\pi\sigma_0. \quad (6)$$

For sufficiently small particles, absorption dominates over radiative corrections, so that we can overlook terms proportional to $|\alpha|^2$ in Eqs. (3)–(5). Then, we find the closed-form expressions

$$P_D^{\text{rad}} = \frac{\hbar a^3}{60\pi^2 c^3 \sigma_0} \left[2\Omega^6 + 5\Omega^4 \theta_1^2 + 3\Omega^2 \theta_1^4 + \frac{5}{14}(\theta_1^6 - \theta_0^6) \right] \quad (7)$$

and

$$M_D = \frac{-\hbar a^3 \Omega}{120\pi^2 c^3 \sigma_0} [6\Omega^4 + 10\Omega^2 \theta_1^2 + \theta_0^4 + 3\theta_1^4], \quad (8)$$

where the subscript D refers to the Drude model and

$$\theta_j = 2\pi k_B T_j / \hbar.$$

Equations (7) and (8) show that vacuum friction is always producing stopping ($M\Omega < 0$), whereas the balance of radiation exchange between particle and free space can change sign depending on their relative temperatures. The general trend of these expressions is shown in Fig. 2(b). At low Ω , the torque scales as Ω , whereas a steeper Ω^5 dependence is observed at faster velocities. Interestingly, a nonzero torque $M \propto \Omega^5$ is predicted at $T_0 = T_1 = 0$, despite the axial symmetry of the particle.

Equilibrium temperature.—The power absorbed by the particle in the form of thermal heating P^{abs} can be obtained from energy conservation, expressed by the identity $-M\Omega = P^{\text{rad}} + P^{\text{abs}}$, where the left-hand side represents mechanical energy dissipation (stopping power). Using Eqs. (7) and (8), we find

$$P_D^{\text{abs}} = \frac{\hbar a^3}{120\pi^2 c^3 \sigma_0} \left[2\Omega^6 + \Omega^2(\theta_0^4 - 3\theta_1^4) + \frac{5}{7}(\theta_0^6 - \theta_1^6) \right]. \quad (9)$$

The particle equilibrium temperature is determined by the condition $P^{\text{abs}} = 0$, and it is stable because $\partial P^{\text{abs}}/\partial T_1 < 0$ [this inequality is obvious from Eq. (9), but it can be easily derived in the general case from Eqs. (3)–(5)]. Unlike conventional friction of a spinning object immersed in

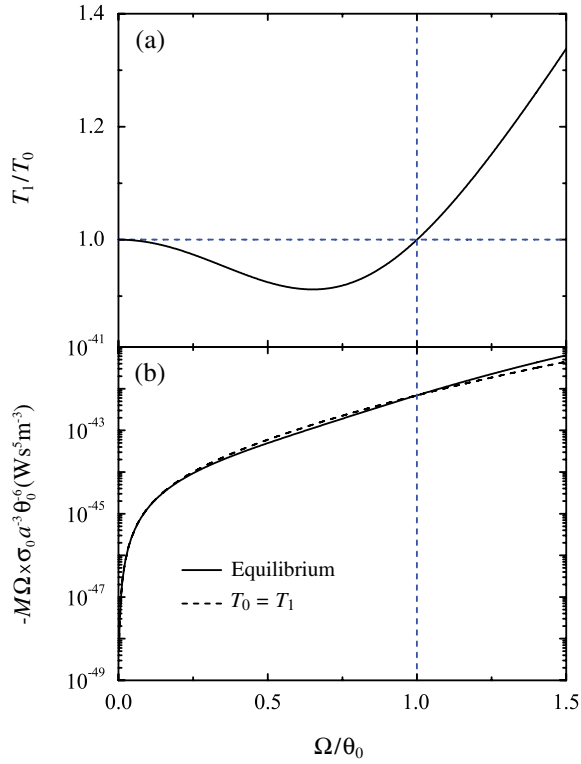


FIG. 2 (color online). Equilibrium temperature and stopping of a metallic sphere. (a) Normalized particle temperature at equilibrium (T_1/T_0) as a function of Ω/θ_0 , where $\theta_0 = 2\pi k_B T_0/\hbar$ (see Fig. 1). (b) Universal normalized stopping power both at equilibrium temperatures (solid curve) and at equal temperatures ($T_0 = T_1$, broken curve).

a fluid, vacuum friction is not always leading to particle heating, as shown in Fig. 2(a) from the solution of $P_D^{\text{abs}} = 0$. Actually, $T_1 < T_0$ for finite temperatures and rotation velocities below $\Omega = \theta_0$, whereas particle heating occurs at higher Ω . The crossing point between these two types of behavior is independent of particle size a and conductivity σ_0 .

At $T_0 = 0$, we find $\theta_1 \approx 0.867 \Omega$, so that the Ω^5 dependence of M_D is maintained with the particle at equilibrium temperature. The loss of mechanical energy is then fully converted into a radiated power $P_D^{\text{rad}} \approx 0.013 \hbar a^3 \Omega^6 / c^3 \sigma_0$.

It should be noted that having the particle at equilibrium temperature or at the same temperature as the vacuum results in significant differences in the stopping power [Fig. 2(b), calculated from Eqs. (6)–(9)].

Emission spectra.—The probability of emitting photons at frequency ω is given by $\Gamma(\omega) - \Gamma(-\omega)$ [see Eq. (4)], which is normalized per unit of emission-frequency range. The emission profile at low rotation velocities ($\Omega = 0.05\theta_0$ curve in Fig. 3) mimics the absorption spectrum from a static cold particle (dashed curve), also peaked around $\hbar\omega \approx 5k_B T_1$ for Drude spheres. However, the maximum of emission is driven by Ω for faster rotations

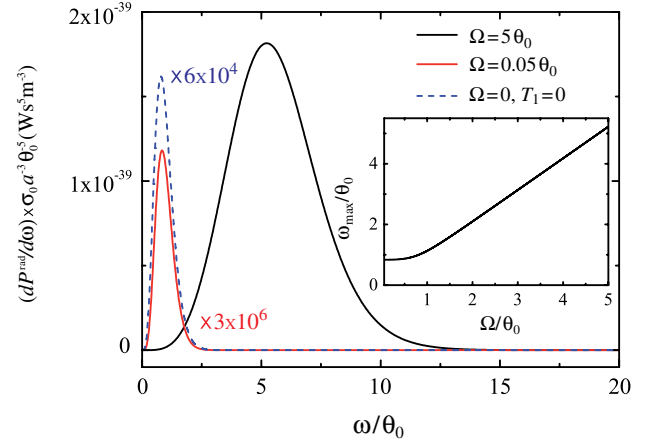


FIG. 3 (color online). Power spectrum $dP^{\text{rad}}/d\omega = \hbar\omega[\Gamma(\omega) - \Gamma(-\omega)]$ [see Eq. (4)] radiated by a metallic spinning particle for various rotation frequencies. Solid curves: emission at equilibrium temperatures. Dashed curve: absorption by a particle at rest and $T_1 = 0$. The emitted-photon frequency ω is normalized to $\theta_0 = 2\pi k_B T_0/\hbar$. The inset shows the frequency of maximum emission at equilibrium as a function of Ω/θ_0 .

(see inset and $\Omega = 5\theta_0$ curve in Fig. 3), thus signaling a significant departure from standard black-body theory.

Stopping time.—At low rotation velocity and finite temperature, the frictional torque acting on a metallic particle is proportional to Ω [see Eq. (8)]. The correction to the particle equilibrium temperature [$\theta_1 \approx \theta_0 - (7/15)\Omega^2/\theta_0$] can be then neglected to first order in Ω , so the torque becomes $M \approx -\beta\Omega$, where $\beta = \hbar a^3 \theta_0^4 / 30\pi^2 c^3 \sigma_0$. From Newton's second law, we find an $\Omega(t) = \Omega(0) \exp(-t/\tau)$ time dependence of the rotation velocity, where $\tau = I/\beta$ is the characteristic stopping time and I is the moment of inertia. For a spherical Drude particle, we find

$$\tau = \frac{(\hbar c)^3}{\pi} \frac{\rho a^2 \sigma_0}{(k_B T_0)^4}, \quad (10)$$

where ρ is the particle density.

Graphite particles are abundant in interstellar dust [15], so we focus on them as an important case to study the rotation stopping time. The frequency-dependent dielectric function of graphite is taken from optical data [16], tabulated for different particle sizes, which differ due to nonlocal corrections. The low- ω behavior is well approximated by the Drude model with $\sigma_0 = 2.3 \times 10^4 (2.0 \times 10^5) \Omega^{-1} \text{m}^{-1}$ for spherical particles of radius $a = 10(100)$ nm, where the response has been averaged over different crystal orientations. Plugging this into Eq. (10), we obtain the results shown in Fig. 4 by broken lines. Interband transitions become important in the response of graphite at frequencies above $\hbar\omega \sim 10^{-2}$ eV, so we expect a deviation from Drude behavior at temperatures above ~ 100 K in this material. This is indeed confirmed by numerically integrating Eq. (5) with the full tabulated response of graphite to obtain τ (Fig. 4, solid curves). For the particle sizes under

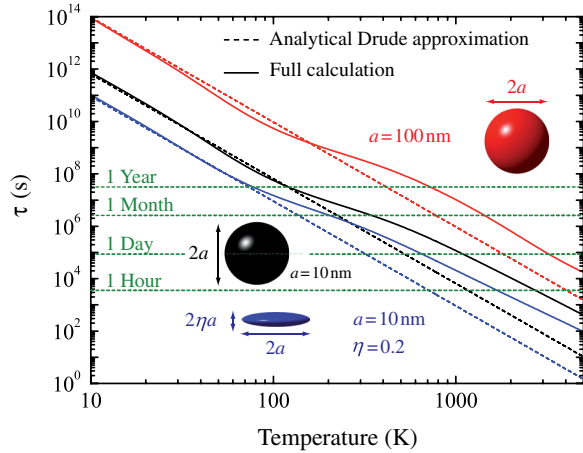


FIG. 4 (color online). Characteristic stopping time of spinning graphite particles as a function of vacuum temperature. Solid curves: full calculation using measured dielectric functions for the graphite particles [16]. Broken curves: analytical Drude approximation [Eq. (10)]. Various particle sizes and shapes are considered: spheres of radius 10 nm and 100 nm, and an oblate ellipsoid of radius 10 nm and aspect ratio $\eta = 0.2$. Low rotation velocities $\Omega \ll k_B T_0 / \hbar$ are assumed (e.g., $\Omega \ll 21$ GHz at $T_0 = 1$ K).

consideration, stopping times are small on cosmic scales within the plotted range of temperatures, which are often encountered in hot dust regions [15]. In cooler areas ($T_0 = 2.7$ K), 100 nm graphite particles have a stopping time $\tau \sim 0.6$ billion years.

Dust particles can adopt nonspherical shapes. In particular, for oblate ellipsoids Eq. (6) [$\text{Im}\{\alpha(\omega)\}$] must be corrected by a factor $\eta/9L^2$, where η is the aspect ratio (see inset in Fig. 4) and L is the depolarization factor for equatorial polarization, approximately linear in η [17]. Also, L is linear in η , thus leading to a $\tau \propto \eta^2$ dependence for fixed radius. We show in Fig. 4 the case $a = 10$ nm and $\eta = 0.2$, which exhibits a significant reduction in τ compared to spherical particles of the same radius. In a related context, translational motion leads to thermal drag [18], only at nonzero temperature and with similar stopping times.

Concluding remarks.—The present results can be relevant to study the distribution of rotation velocities of cosmic nanoparticles, which could be eventually examined through measurements of rotational frequency shifts [19]. Besides, relatively small stopping times are predicted for graphite nanoparticles, which ask for experimental corroboration (for example, using *in vacuo* optical trapping setups). By analogy to the Purcell effect [20], the frictional torque can be altered due to the presence of physical boundaries that modify the density of states appearing in Eq. (4), thus opening new possibilities for controlling the degree of friction (e.g., the torque can be strongly reduced

at low temperature and small rotation frequency by placing the particle inside a metallic cavity, which produces a threshold of ρ^0 in ω).

This work has been supported by the Spanish MICINN (MAT2007-66050 and Consolider NanoLight.es). A. M. acknowledges financial support through FPU from ME.

*Corresponding author.

J.G.deAbajo@csic.es

- [1] K. Briggs, *Aust. J. Phys.* **41**, 629 (1988).
- [2] D. Park, *Phys. Rev.* **99**, 1324 (1955).
- [3] F. S. Chute, *IEEE Trans. Antennas Propag.* **15**, 585 (1967).
- [4] O. Kenneth and S. Nussinov, *Phys. Rev. D* **65**, 085014 (2002).
- [5] M. Kardar and R. Golestanian, *Rev. Mod. Phys.* **71**, 1233 (1999).
- [6] S. H. Tao *et al.*, *Opt. Express* **13**, 7726 (2005).
- [7] J. B. Pendry, *J. Phys. Condens. Matter* **9**, 10301 (1997).
- [8] T. G. Philbin and U. Leonhardt, *New J. Phys.* **11**, 033035 (2009); G. V. Dedkov and A. A. Kyasov, *Surf. Sci.* **604**, 562 (2010); J. B. Pendry, *New J. Phys.* **12**, 033028 (2010); U. Leonhardt, *New J. Phys.* **12**, 068001 (2010); J. B. Pendry, *New J. Phys.* **12**, 068002 (2010).
- [9] Y. Pomeau, *J. Stat. Phys.* **121**, 1083 (2005); *Europhys. Lett.* **74**, 951 (2006).
- [10] See supplementary material at <http://link.aps.org/supplemental/10.1103/PhysRevLett.105.113601> for the FDT and the derivation of Eqs. (3)–(5).
- [11] H. C. van de Hulst, *Light Scattering by Small Particles* (Dover, New York, 1981).
- [12] From a quantum mechanical point of view, the lowest-order coupling Hamiltonian producing vacuum friction includes terms with simultaneous changes in (i) the rotational state of the particle ($m \rightarrow m \pm 1$ jumps in the azimuthal quantum number), (ii) the internal state of the particle, and (iii) the number of vacuum photon states [10]. In nonabsorbing spheres, no such matrix elements exist because internal excitations are not available.
- [13] A. Manjavacas and F. J. García de Abajo (to be published); magnetic polarization can play a small role at large temperatures in the left part of Fig. 4.
- [14] N. W. Ashcroft and N. D. Mermin, *Solid State Physics* (Harcourt College Publishers, New York, 1976).
- [15] F. Hoyle and N. C. Wickramasinghe, *Mon. Not. R. Astron. Soc.* **124**, 417 (1962).
- [16] B. T. Draine, *Astrophys. J.* **598**, 1026 (2003).
- [17] V. Myroshnychenko *et al.*, *Chem. Soc. Rev.* **37**, 1792 (2008).
- [18] V. Mkrтчian, V. A. Parsegian, R. Podgornik, and W. M. Saslow, *Phys. Rev. Lett.* **91**, 220801 (2003).
- [19] I. Bialynicki-Birula and Z. Bialynicka-Birula, *Phys. Rev. Lett.* **78**, 2539 (1997); M. Michalski, W. Hüttner, and H. Schimming, *Phys. Rev. Lett.* **95**, 203005 (2005).
- [20] E. M. Purcell, *Phys. Rev.* **69**, 681 (1946).